JOURNAL OF SANDWICH STRUCTURES & MATERIALS

Article

Journal of Sandwich Structures and Materials
14(5) 505–524

DOI: 10.1177/1099636212449083
jsm.sagepub.com
SAGE

Analysis of sandwich plates by radial basis functions collocation, according to Murakami's Zig-Zag theory

António Joaquim Mendes Ferreira[1], Carla Maria da Cunha Roque[2], Erasmo Carrera[3], Maria Cinefra[3] and Olivier Polit[4]

Abstract

In this article, the static analysis of sandwich plates is performed by radial basis functions collocation, according to the Murakami's Zig-Zag function theory. The Murakami's Zig-Zag function theory accounts for through-the-thickness deformation, by considering a Zig-Zag evolution of the transverse displacement with the thickness coordinate. The equations of motion and the boundary conditions are obtained by the Carrera's unified formulation, and further interpolated by collocation with radial basis functions.

Keywords

Sandwich, Zig-Zag theories, radial basis functions, unified formulation

Introduction

This so-called zig-zag (ZZ) effect in sandwich structures or layered composites is a result of the discontinuity of mechanical properties between faces and core at the interfaces (Figure 1). An historical review on ZZ theories has been provided by Carrera [1].

[1]Departamento de Engenharia Mecânica, Faculdade de Engenharia da Universidade do Porto, Rua Dr. Roberto Frias, Porto, Portugal
[2]INEGI, Faculdade de Engenharia da Universidade do Porto, Rua Dr. Roberto Frias, Porto, Portugal
[3]Departament of Aeronautics and Aerospace Engineering, Politecnico di Torino, Corso Duca degli Abruzzi, Torino, Italy
[4]Université Paris Ouest - Nanterre, 50 rue de Sevres, Ville d'Avray, France

Corresponding author:
António Joaquim Mendes Ferreira, Departamento de Engenharia Mecânica, Faculdade de Engenharia da Universidade do Porto, Rua Dr. Roberto Frias, 4200-465 Porto, Portugal.
Email: ferreira@fe.up.pt

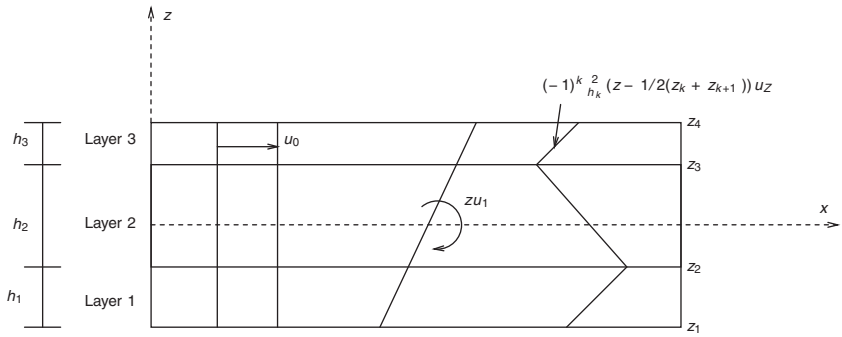

Figure 1. Scheme of the zig-zag assumptions for a three-layered laminate.

The classical theories such as Kirchhoff [2] or Reissner-Mindlin [3,4] type theories (to trace accurate responses of sandwich structures, see the books by Zenkert [5] and Vinson [6]) are not adequate to model such discontinuities.

The ZZ effect can be captured by the layerwise theories which typically assume independent degrees-of-freedom per layer. Unfortunately the computation can be prohibitive. The layerwise theories are reviewed in Burton and Noor [7], Noor et al. [8], Altenbach [9], Librescu and Hause [10], Vinson [11] and Demasi [12].

In order to overcome the computational cost of the layerwise theories, Murakami [13] proposed a zig-zag function ZZF that is able to reproduce the slope discontinuity. Equivalent single layer models with only displacement unknowns can be developed on the basis of ZZF. A review of the application of ZZF in plates and shells was presented by Carrera [14,15,15–17]. Some relevant papers on the analysis of sandwich structures were presented in Beluouettar et al. [18], Frostig [19] and Frostig and Rabinovich [20].

The present article applies the Murakami's ZZF to bending, vibration and buckling analysis of sandwich plates by collocation with radial basis functions. A radial basis function, $\phi(\|x - x_j\|)$ is a spline that depends on the Euclidian distance between distinct data centers $x_j, j = 1, 2, \ldots, N \in \mathbb{R}^n$, also called nodal or collocation points. We use the so-called unsymmetrical Kansa method, that was introduced by Kansa [21]. The use of radial basis function for the analysis of structures and materials has been previously studied by numerous authors [22–36]. The authors have recently applied the radial basis function (RBF) collocation to the static deformations of composite beams and plates [37–39].

In this article it is investigated for the first time how the unified formulation (UF) can be combined with radial basis functions to the analysis of thin and thick sandwich plates, using the MZZF, allowing for through-the-thickness deformations. The quality of the present method in predicting static deformations, free vibrations and buckling loads of thin and thick sandwich plates is compared and discussed with other methods in some numerical examples.

Applying the unified formulation to MZZF

The UF proposed by Carrera [14,40–42], also known as CUF, is a powerful framework for the analysis of beams, plates and shells. This formulation has been applied in several finite element analysis, either using the principle of virtual displacements, or by using the Reissner's Mixed Variational theorem. The stiffness matrix components, the external force terms or the inertia terms can be obtained directly with this UF, irrespective of the shear deformation theory being considered.

In this section the Carrera's UF [14,40–42] is briefly reviewed. It is shown how to obtain the fundamental nuclei, which allows the derivation of the equations of motion and boundary conditions, in weak form for the finite element analysis; and in strong form for the present RBF collocation.

The MZZF theory

Let us consider a sandwich plate composed of three perfectly bonded layers, being z the thickness coordinate of the whole plate while z_k is the layer thickness coordinate (Figure 1). a and h are length and thickness of the square sandwich plate, respectively. The adimensioned layer coordinate $\zeta_k = (2z_k)/h_k$ is further introduced (h_k is the thickness of the kth layer). The Murakami's zig-zag function $Z(z)$ was defined according to the following formula [13]

$$Z(z) = (-1)^k \zeta_z \tag{1}$$

$Z(z)$ has the following properties:

1. It is a piece-wise linear function of layer coordinates z_k,
2. $Z(z)$ has unit amplitude for the whole layers,
3. the slope $Z'(z) = \frac{dZ}{dz}$ assumes opposite sign between two-adjacent layers. Its amplitude is layer thickness independent.

A possible FSDT theory has been investigated by Carrera [15] and Demasi [16], ignoring the through-the-thickness deformations

$$u = u_0 + zu_1 + (-1)^k \frac{2}{h_k}\left(z - \frac{1}{2}(z_k + z_{k+1})\right)u_Z \tag{2}$$

$$v = v_0 + zv_1 + (-1)^k \frac{2}{h_k}\left(z - \frac{1}{2}(z_k + z_{k+1})\right)v_Z \tag{3}$$

$$w = w_0 \tag{4}$$

A refinement of FSDT by inclusion of ZZ effects and transverse normal strains was introduced in Murakami's original ZZF, defined by the following displacement field

$$u = u_0 + zu_1 + (-1)^k \frac{2}{h_k}\left(z - \frac{1}{2}(z_k + z_{k+1})\right)u_Z \tag{5}$$

$$v = v_0 + zv_1 + (-1)^k \frac{2}{h_k}\left(z - \frac{1}{2}(z_k + z_{k+1})\right)v_Z \tag{6}$$

$$w = w_0 + zw_1 + (-1)^k \frac{2}{h_k}\left(z - \frac{1}{2}(z_k + z_{k+1})\right)w_Z \tag{7}$$

where z_k, z_{k+1} are the bottom and top z-coordinates at each layer. The additional degrees of freedom u_Z, v_z have a meaning of displacement, and its amplitude is layer independent.

Governing equations and boundary conditions in the framework of unified formulation

Although one can use the UF for one-layer , isotropic plate, a multi-layered plate with N_l layers is considered. The principle of virtual displacements (PVD) for the pure-mechanical case reads

$$\sum_{k=1}^{N_l} \int_{\Omega_k} \int_{A_k} \left\{ \delta\epsilon_{pG}^{k\,T} \sigma_{pC}^k + \delta\epsilon_{nG}^{k\,T} \sigma_{nC}^k \right\} \mathrm{d}\Omega_k \mathrm{d}z = \sum_{k=1}^{N_l} \delta L_e^k \tag{8}$$

where Ω_k and A_k are the integration domains in plane (x,y) and z direction, respectively. Here, k indicates the layer and T the transpose of a vector, and δL_e^k is the external work for the kth layer. G means geometrical relations and C constitutive equations.

The steps to obtain the governing equations are:

- Substitution of the geometrical relations (subscript G)
- Substitution of the appropriate constitutive equations (subscript C)
- Introduction of the unified formulation

Stresses and strains are separated into in-plane and normal components, denoted respectively by the subscripts p and n. The mechanical strains in the kth layer can be related to the displacement field $\mathbf{u}^k = \{u_x^k, u_y^k, u_z^k\}$ via the geometrical relations

$$\begin{aligned} \epsilon_{pG}^k &= [\epsilon_{xx}, \epsilon_{yy}, \gamma_{xy}]^{kT} = \mathbf{D}_p^k \mathbf{u}^k \,, \\ \epsilon_{nG}^k &= [\gamma_{xz}, \gamma_{yz}, \epsilon_{zz}]^{kT} = (\mathbf{D}_{np}^k + \mathbf{D}_{nz}^k)\, \mathbf{u}^k \,, \end{aligned} \tag{9}$$

wherein the differential operator arrays are defined as follows

$$\mathbf{D}_p^k = \begin{bmatrix} \partial_x & 0 & 0 \\ 0 & \partial_y & 0 \\ \partial_y & \partial_x & 0 \end{bmatrix}, \quad \mathbf{D}_{np}^k = \begin{bmatrix} 0 & 0 & \partial_x \\ 0 & 0 & \partial_y \\ 0 & 0 & 0 \end{bmatrix}, \quad \mathbf{D}_{nz}^k = \begin{bmatrix} \partial_z & 0 & 0 \\ 0 & \partial_z & 0 \\ 0 & 0 & \partial_z \end{bmatrix}, \tag{10}$$

The deformations are obtained, for each layer k, as

$$\epsilon^k_{xx} = \frac{\partial u^k}{\partial x} = \frac{\partial u_0}{\partial x} + z\frac{\partial u_1}{\partial x} + (-1)^k \frac{2}{h_k}\left(z - \frac{1}{2}(z_k + z_{k+1})\right)\frac{\partial u_Z}{\partial x} \tag{11}$$

$$\epsilon^k_{yy} = \frac{\partial v^k}{\partial y} = \frac{\partial v_0}{\partial y} + z\frac{\partial v_1}{\partial y} + (-1)^k \frac{2}{h_k}\left(z - \frac{1}{2}(z_k + z_{k+1})\right)\frac{\partial v_Z}{\partial y} \tag{12}$$

$$\epsilon^k_{zz} = \frac{\partial w^k}{\partial z} = w_1 + (-1)^k \frac{2}{h_k} w_Z \tag{13}$$

$$\begin{aligned}\gamma^k_{xy} = \frac{\partial u^k}{\partial y} + \frac{\partial v^k}{\partial x} = \frac{\partial u_0}{\partial y} + \frac{\partial v_0}{\partial x} + z\left(\frac{\partial u_1}{\partial y} + \frac{\partial v_1}{\partial x}\right) \\ + (-1)^k \frac{2}{h_k}\left(z - \frac{1}{2}(z_k + z_{k+1})\right)\left(\frac{\partial u_Z}{\partial y} + \frac{\partial v_Z}{\partial x}\right)\end{aligned} \tag{14}$$

$$\begin{aligned}\gamma^k_{xz} = \frac{\partial u^k}{\partial z} + \frac{\partial w^k}{\partial x} = u_1 + (-1)^k \frac{2}{h_k} u_Z + \frac{\partial w_0}{\partial x} + z\frac{\partial w_1}{\partial x} \\ + (-1)^k \frac{2}{h_k}\left(z - \frac{1}{2}(z_k + z_{k+1})\right)\frac{\partial w_Z}{\partial x}\end{aligned} \tag{15}$$

$$\begin{aligned}\gamma^k_{yz} = \frac{\partial v^k}{\partial z} + \frac{\partial w^k}{\partial y} = v_1 + (-1)^k \frac{2}{h_k} v_Z + \frac{\partial w_0}{\partial y} + z\frac{\partial w_1}{\partial y} \\ + (-1)^k \frac{2}{h_k}\left(z - \frac{1}{2}(z_k + z_{k+1})\right)\frac{\partial w_Z}{\partial y}\end{aligned} \tag{16}$$

The 3D constitutive equations are given as

$$\begin{aligned}\sigma^k_{pC} &= \mathbf{C}^k_{pp}\,\epsilon^k_{pG} + \mathbf{C}^k_{pn}\,\epsilon^k_{nG} \\ \sigma^k_{nC} &= \mathbf{C}^k_{np}\,\epsilon^k_{pG} + \mathbf{C}^k_{nn}\,\epsilon^k_{nG}\end{aligned} \tag{17}$$

with

$$\begin{aligned}\mathbf{C}^k_{pp} &= \begin{bmatrix} C_{11} & C_{12} & C_{16} \\ C_{12} & C_{22} & C_{26} \\ C_{16} & C_{26} & C_{66} \end{bmatrix} \quad \mathbf{C}^k_{pn} = \begin{bmatrix} 0 & 0 & C_{13} \\ 0 & 0 & C_{23} \\ 0 & 0 & C_{36} \end{bmatrix} \\ \mathbf{C}^k_{np} &= \begin{bmatrix} 0 & 0 & 0 \\ 0 & 0 & 0 \\ C_{13} & C_{23} & C_{36} \end{bmatrix} \quad \mathbf{C}^k_{nn} = \begin{bmatrix} C_{55} & C_{45} & 0 \\ C_{45} & C_{44} & 0 \\ 0 & 0 & C_{33} \end{bmatrix}\end{aligned} \tag{18}$$

According to the UF by Carrera, the three displacement components u_x, u_y and u_z and their relative variations can be modelled as

$$(u_x, u_y, u_z) = F_\tau\ (u_{x\tau}, u_{y\tau}, u_{z\tau}) \quad (\delta u_x, \delta u_y, \delta u_z) = F_s\ (\delta u_{xs}, \delta u_{ys}, \delta u_{zs}) \tag{19}$$

with Taylor expansions from first up to 4th order: $F_0 = z^0 = 1$, $F_1 = z^1 = z, \ldots, F_N = z^N, \ldots, F_4 = z^4$ if an Equivalent Single Layer (ESL) approach is used.

Resorting to the displacement field in equation (5), we choose vectors $F_t = [1 \quad z \quad (-1)^k \frac{2}{h_k}\left(z - \frac{1}{2}(z_k + z_{k+1})\right)]$ for displacements u, v, w. We then obtain all terms of the equations of motion by integrating through the thickness direction.

It is interesting to note that under this combination of the UF and RBF collocation, the collocation code depends only on the choice of F_t, in order to solve this type of problems. We designed a MATLAB code that just by changing F_t can analyze static deformations, free vibrations and buckling loads for any type of C° shear deformation theory. An obvious advantage of the present methodology is that the tedious derivation of the equations of motion and boundary conditions for a particular shear deformation theory is no longer an issue, as this MATLAB code does all that work for us.

The assembling procedures on layer k for ESL approach is shown in Figure 2.

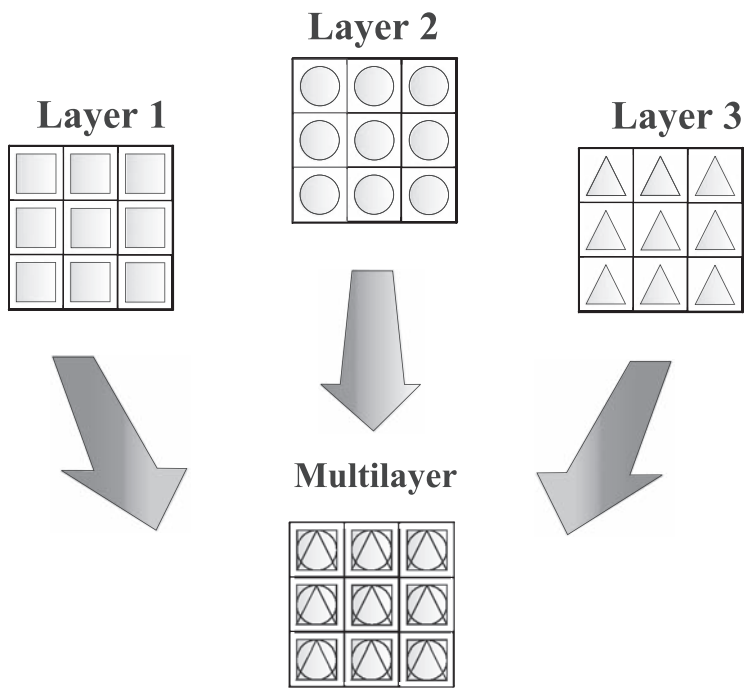

Figure 2. Assembling procedure for ESL approach.
ESL: equivalent single layer.

Substituting the geometrical relations, the constitutive equations and the UF into the variational statement PVD, for the kth layer, one has

$$\int_{\Omega_k}\int_{A_k}\Big[(\mathbf{D}_p^k\ F_s\delta\mathbf{u}_s^k)^T(\mathbf{C}_{pp}^k\mathbf{D}_p^k\ F_\tau\mathbf{u}_\tau^k+\mathbf{C}_{pn}^k(\mathbf{D}_{n\Omega}^k+\mathbf{D}_{nz}^k)F_\tau\mathbf{u}_\tau^k)$$
$$+((\mathbf{D}_{n\Omega}^k+\mathbf{D}_{nz}^k)F_s\delta\mathbf{u}_s^k)^T(\mathbf{C}_{np}^k\mathbf{D}_p^k\ F_\tau\mathbf{u}_\tau^k+\mathbf{C}_{nn}^k(\mathbf{D}_{n\Omega}^k+\mathbf{D}_{nz}^k)F_\tau\mathbf{u}_\tau^k)\Big]\mathrm{d}\Omega_k\mathrm{d}z=\delta L_e^k \tag{20}$$

At this point, the formula of integration by parts is applied

$$\int_{\Omega_k}\big((\mathbf{D}_\Omega)\delta\mathbf{a}^k\big)^T\mathbf{a}^k\mathrm{d}\Omega_k=-\int_{\Omega_k}\delta\mathbf{a}^{kT}\big((\mathbf{D}_\Omega^T)\mathbf{a}^k\big)\mathrm{d}\Omega_k+\int_{\Gamma_k}\delta\mathbf{a}^{kT}\big((\mathbf{I}_\Omega)\mathbf{a}^k\big)\mathrm{d}\Gamma_k \tag{21}$$

where $\mathbf{I}_\Omega$ matrix is obtained applying the *Gradient theorem*

$$\int_\Omega\frac{\partial\psi}{\partial x_i}d\upsilon=\oint_\Gamma n_i\psi\mathrm{d}s \tag{22}$$

being n_i the components of the normal $\widehat{n}$ to the boundary along the direction i. After integration by parts, the governing equations and boundary conditions for the plate in the mechanical case are obtained

$$\int_{\Omega_k}\int_{A_k}(\ \delta\mathbf{u}_s^k)^T\Big[\Big(\big(-\mathbf{D}_p^k\big)^T\big(\mathbf{C}_{pp}^k(\mathbf{D}_p^k)\ +\mathbf{C}_{pn}^k(\mathbf{D}_{n\Omega}^k+\mathbf{D}_{nz}^k)$$
$$+\big(-\mathbf{D}_{n\Omega}^k+\mathbf{D}_{nz}^k\big)^T\big(\mathbf{C}_{np}^k(\mathbf{D}_p^k)+\mathbf{C}_{nn}^k(\mathbf{D}_{n\Omega}^k+\mathbf{D}_{nz}^k)\big)\Big)\mathbf{F}_\tau\mathbf{F}_s\mathbf{u}_\tau^k\Big]\mathrm{d}x\mathrm{d}y\mathrm{d}z$$
$$+\int_{\Omega_k}\int_{A_k}(\ \delta\mathbf{u}_s^k)^T\Big[\Big(\mathbf{I}_p^{kT}\big(\mathbf{C}_{pp}^k(\mathbf{D}_p^k)\ +\mathbf{C}_{pn}^k(\mathbf{D}_{n\Omega}^k+\mathbf{D}_{nz}^k)\big)$$
$$+\mathbf{I}_{np}^{kT}\big(\mathbf{C}_{np}^k(\mathbf{D}_p^k)\ +\mathbf{C}_{nn}^k(\mathbf{D}_{n\Omega}^k+\mathbf{D}_{nz}^k)\big)\Big)\mathbf{F}_\tau\mathbf{F}_s\mathbf{u}_\tau^k\Big]\mathrm{d}x\mathrm{d}y\mathrm{d}z=\int_{\Omega_k}\delta\mathbf{u}_s^{kT}F_s\mathbf{p}_u^k\mathrm{d}\Omega_k. \tag{23}$$

where $\mathbf{I}_p^k$ and $\mathbf{I}_{np}^k$ depend on the boundary geometry

$$\mathbf{I}_p^k=\begin{bmatrix}n_x&0&0\\0&n_y&0\\n_y&n_x&0\end{bmatrix},\quad\mathbf{I}_{np}^k=\begin{bmatrix}0&0&n_x\\0&0&n_y\\0&0&0\end{bmatrix}. \tag{24}$$

The normal to the boundary of domain Ω is

$$\widehat{\mathbf{n}}=\begin{bmatrix}n_x\\n_y\end{bmatrix}=\begin{bmatrix}\cos(\varphi_x)\\\cos(\varphi_y)\end{bmatrix} \tag{25}$$

where φ_x and φ_y are the angles between the normal $\widehat{n}$ and the direction x and y, respectively.

The governing equations for a multi-layered plate subjected to mechanical loadings are

$$\delta \mathbf{u}_s^{k\,T} : \quad \mathbf{K}_{uu}^{k\tau s}\,\mathbf{u}_\tau^k = \mathbf{P}_{u\tau}^k \tag{26}$$

where the fundamental nucleus $\mathbf{K}_{uu}^{k\tau s}$ is obtained as

$$\begin{aligned}\mathbf{K}_{uu}^{k\tau s} = &\Big[\big(-\mathbf{D}_p^k\big)^T\big(\mathbf{C}_{pp}^k(\mathbf{D}_p^k) + \mathbf{C}_{pn}^k(\mathbf{D}_{n\Omega}^k + \mathbf{D}_{nz}^k\big)\\ &+ \big(-\mathbf{D}_{n\Omega}^k + \mathbf{D}_{nz}^k\big)^T\big(\mathbf{C}_{np}^k(\mathbf{D}_p^k) + \mathbf{C}_{nn}^k(\mathbf{D}_{n\Omega}^k + \mathbf{D}_{nz}^k)\big)\Big]\mathbf{F}_\tau\mathbf{F}_s\end{aligned} \tag{27}$$

and the corresponding Neumann-type boundary conditions on Γ_k are

$$\mathbf{\Pi}_d^{k\tau s}\,\mathbf{u}_\tau^k = \mathbf{\Pi}_d^{k\tau s}\,\mathbf{u}_\tau^{\,k}\,, \tag{28}$$

where

$$\begin{aligned}\mathbf{\Pi}_d^{k\tau s} = &\Big[\mathbf{I}_p^{kT}\big(\mathbf{C}_{pp}^k(\mathbf{D}_p^k) + \mathbf{C}_{pn}^k(\mathbf{D}_{n\Omega}^k + \mathbf{D}_{nz}^k)\big)\\ &+ \mathbf{I}_{np}^{kT}\big(\mathbf{C}_{np}^k(\mathbf{D}_p^k) + \mathbf{C}_{nn}^k(\mathbf{D}_{n\Omega}^k + \mathbf{D}_{nz}^k)\big)\Big]\mathbf{F}_\tau\mathbf{F}_s\end{aligned} \tag{29}$$

and $\mathbf{P}_{u\tau}^k$ are variationally consistent loads with applied pressure.

Fundamental nuclei

The fundamental nuclei in explicit form are then obtained as

$$\begin{aligned}
K_{uu_{11}}^{k\tau s} &= (-\partial_x^\tau\partial_x^s C_{11} - \partial_x^\tau\partial_y^s C_{16} + \partial_z^\tau\partial_z^s C_{55} - \partial_y^\tau\partial_x^s C_{16} - \partial_y^\tau\partial_y^s C_{66})F_\tau F_s\\
K_{uu_{12}}^{k\tau s} &= (-\partial_x^\tau\partial_y^s C_{12} - \partial_x^\tau\partial_x^s C_{16} + \partial_z^\tau\partial_z^s C_{45} - \partial_y^\tau\partial_y^s C_{26} - \partial_y^\tau\partial_x^s C_{66})F_\tau F_s\\
K_{uu_{13}}^{k\tau s} &= (-\partial_x^\tau\partial_z^s C_{13} - \partial_y^\tau\partial_z^s C_{36} + \partial_z^\tau\partial_y^s C_{45} + \partial_z^\tau\partial_x^s C_{55})F_\tau F_s\\
K_{uu_{21}}^{k\tau s} &= (-\partial_y^\tau\partial_x^s C_{12} - \partial_y^\tau\partial_y^s C_{26} + \partial_z^\tau\partial_z^s C_{45} - \partial_x^\tau\partial_x^s C_{16} - \partial_x^\tau\partial_y^s C_{66})F_\tau F_s\\
K_{uu_{22}}^{k\tau s} &= (-\partial_y^\tau\partial_y^s C_{22} - \partial_y^\tau\partial_x^s C_{26} + \partial_z^\tau\partial_z^s C_{44} - \partial_x^\tau\partial_y^s C_{26} - \partial_x^\tau\partial_x^s C_{66})F_\tau F_s\\
K_{uu_{23}}^{k\tau s} &= (-\partial_y^\tau\partial_z^s C_{23} - \partial_x^\tau\partial_z^s C_{36} + \partial_z^\tau\partial_y^s C_{44} + \partial_z^\tau\partial_x^s C_{45})F_\tau F_s\\
K_{uu_{31}}^{k\tau s} &= (\partial_z^\tau\partial_x^s C_{13} + \partial_z^\tau\partial_y^s C_{36} - \partial_y^\tau\partial_z^s C_{45} - \partial_x^\tau\partial_z^s C_{55})F_\tau F_s\\
K_{uu_{32}}^{k\tau s} &= (\partial_z^\tau\partial_y^s C_{23} + \partial_z^\tau\partial_x^s C_{36} - \partial_y^\tau\partial_z^s C_{44} - \partial_x^\tau\partial_z^s C_{45})F_\tau F_s\\
K_{uu_{33}}^{k\tau s} &= (\partial_z^\tau\partial_z^s C_{33} - \partial_y^\tau\partial_y^s C_{44} - \partial_y^\tau\partial_x^s C_{45} - \partial_x^\tau\partial_y^s C_{45} - \partial_x^\tau\partial_x^s C_{55})F_\tau F_s
\end{aligned} \tag{30}$$

$$
\begin{aligned}
\Pi_{11}^{k\tau s} &= (n_x\partial_x^s C_{11} + n_x\partial_y^s C_{16} + n_y\partial_x^s C_{16} + n_y\partial_y^s C_{66})F_\tau F_s \\
\Pi_{12}^{k\tau s} &= (n_x\partial_y^s C_{12} + n_x\partial_x^s C_{16} + n_y\partial_y^s C_{26} + n_y\partial_x^s C_{66})F_\tau F_s \\
\Pi_{13}^{k\tau s} &= (n_x\partial_z^s C_{13} + n_y\partial_z^s C_{36})F_\tau F_s \\
\Pi_{21}^{k\tau s} &= (n_y\partial_x^s C_{12} + n_y\partial_y^s C_{26} + n_x\partial_x^s C_{16} + n_x\partial_y^s C_{66})F_\tau F_s \\
\Pi_{22}^{k\tau s} &= (n_y\partial_y^s C_{22} + n_y\partial_x^s C_{26} + n_x\partial_y^s C_{26} + n_x\partial_x^s C_{66})F_\tau F_s \\
\Pi_{23}^{k\tau s} &= (n_y\partial_z^s C_{23} + n_x\partial_z^s C_{36})F_\tau F_s \\
\Pi_{31}^{k\tau s} &= (n_y\partial_z^s C_{45} + n_x\partial_z^s C_{55})F_\tau F_s \\
\Pi_{32}^{k\tau s} &= (n_y\partial_z^s C_{44} + n_x\partial_z^s C_{45})F_\tau F_s \\
\Pi_{33}^{k\tau s} &= (n_y\partial_y^s C_{44} + n_y\partial_x^s C_{45} + n_x\partial_y^s C_{45} + n_x\partial_x^s C_{55})F_\tau F_s
\end{aligned} \tag{31}
$$

Dynamic governing equations

The PVD for the dynamic case is expressed as

$$
\sum_{k=1}^{N_l} \int_{\Omega_k} \int_{A_k} \left\{ \delta\epsilon_{pG}^{k\,T} \sigma_{pC}^k + \delta\epsilon_{nG}^{k\,T} \sigma_{nC}^k \right\} \mathrm{d}\Omega_k \mathrm{d}z = \sum_{k=1}^{N_l} \int_{\Omega_k} \int_{A_k} \rho^k \delta\mathbf{u}^{k\,T} \ddot{\mathbf{u}}^k \mathrm{d}\Omega_k \mathrm{d}z + \sum_{k=1}^{N_l} \delta L_e^k \tag{32}
$$

where ρ^k is the mass density of the kth layer and double dots denote acceleration.

By substituting the geometrical relations, the constitutive equations and the UF, we obtain the following governing equations

$$
\delta\mathbf{u}_s^{k\,T} : \quad \mathbf{K}_{uu}^{k\tau s}\,\mathbf{u}_\tau^k = \mathbf{M}^{k\tau s}\ddot{\mathbf{u}}_\tau^k + \mathbf{P}_{u\tau}^k \tag{33}
$$

In the case of free vibrations one has

$$
\delta\mathbf{u}_s^{k\,T} : \quad \mathbf{K}_{uu}^{k\tau s}\,\mathbf{u}_\tau^k = \mathbf{M}^{k\tau s}\ddot{\mathbf{u}}_\tau^k \tag{34}
$$

where $\mathbf{M}^{k\tau s}$ is the fundamental nucleus for the inertial term. The explicit form of that is

$$
M_{11}^{k\tau s} = \rho^k F_\tau F_s; \quad M_{12}^{k\tau s} = 0; \quad M_{13}^{k\tau s} = 0 \tag{35}
$$

$$
M_{21}^{k\tau s} = 0; \quad M_{22}^{k\tau s} = \rho^k F_\tau F_s; \quad M_{23}^{k\tau s} = 0 \tag{36}
$$

$$
M_{31}^{k\tau s} = 0; \quad M_{32}^{k\tau s} = 0; \quad M_{33}^{k\tau s} = \rho^k F_\tau F_s \tag{37}
$$

The geometrical and mechanical boundary conditions are the same of the static case. Because we consider the static case only, the mass terms will be neglected.

The radial basis function method

The static problem

RBF approximations are mesh-free numerical schemes that can exploit accurate representations of the boundary, are easy to implement and can be spectrally accurate. In this section the formulation of a global unsymmetrical collocation RBF-based method to compute elliptic operators is presented.

Consider a linear elliptic partial differential operator L and a bounded region Ω in $\mathbb{R}^n$ with some boundary $\partial\Omega$. In the static problems we seek the computation of displacements **(u)** from the global system of equations

$$\mathcal{L}\mathbf{u} = \mathbf{f} \text{ in } \Omega \tag{38}$$

$$\mathcal{L}_B\mathbf{u} = \mathbf{g} \text{ on } \partial\Omega \tag{39}$$

where $\mathcal{L}$, $\mathcal{L}_B$ are linear operators in the domain and on the boundary, respectively. The right-hand side of equations (38) and (39) represent the external forces applied on the plate and the boundary conditions applied along the perimeter of the plate, respectively. The PDE problem defined in equations (38) and (39) will be replaced by a finite problem, defined by an algebraic system of equations, after the radial basis expansions.

The eigenproblem

The eigenproblem looks for eigenvalues (λ) and eigenvectors **(u)** that satisfy

$$\mathcal{L}\mathbf{u} + \lambda\mathbf{u} = 0 \text{ in } \Omega \tag{40}$$

$$\mathcal{L}_B\mathbf{u} = 0 \text{ on } \partial\Omega \tag{41}$$

As in the static problem, the eigenproblem defined in equations (40) and (41) is replaced by a finite-dimensional eigenvalue problem, based on RBF approximations.

Radial basis functions approximations

The RBF (ϕ) approximation of a function **(u)** is given by

$$\widetilde{\mathbf{u}}(\mathbf{x}) = \sum_{i=1}^{N} \alpha_i \phi(\|x - y_i\|_2), \mathbf{x} \in \mathbb{R}^n \tag{42}$$

where y_i, $i=1,\ldots,N$ is a finite set of distinct points (centers) in $\mathbb{R}^n$. The most common RBFs are

$$\begin{aligned}
\text{Cubic:} &\quad \phi(r) = r^3 \\
\text{Thin plate splines:} &\quad \phi(r) = r^2 \log(r) \\
\text{Wendland functions:} &\quad \phi(r) = (1-r)_+^m p(r) \\
\text{Gaussian:} &\quad \phi(r) = e^{-(cr)^2} \\
\text{Multiquadrics:} &\quad \phi(r) = \sqrt{c^2 + r^2} \\
\text{Inverse multiquadrics:} &\quad \phi(r) = (c^2 + r^2)^{-1/2}
\end{aligned}$$

where the Euclidian distance r is real and non-negative and c is a positive shape parameter. Hardy [43] introduced multiquadrics in the analysis of scattered geographical data. In the 1990's Kansa [21] used multiquadrics for the solution of partial differential equations. Considering N distinct interpolations, and knowing $u(x_j)$, $j=1, 2,\ldots,N$, we find α_i by the solution of a $N \times N$ linear system

$$\mathbf{A}\alpha = \mathbf{u} \tag{43}$$

where $\mathbf{A} = [\phi\,(\|x - y_i\|_2)]_{N\times N}$, $\boldsymbol{\alpha} = [\alpha_1, \alpha_2, \ldots, \alpha_N]^T$ and $\mathbf{u} = [u(x_1), u(x_2), \ldots, u(x_N)]^T$.

Solution of the static problem

The solution of a static problem by radial basis functions considers N_I nodes in the domain and N_B nodes on the boundary, with a total number of nodes $N = N_I + N_B$. We denote the sampling points by $x_i \in \Omega$, $i=1,\ldots,N_I$ and $x_i \in \partial\Omega$, $i=N_I+1,\ldots,N$. At the points in the domain we solve the following system of equations

$$\sum_{i=1}^{N} \alpha_i \mathcal{L}\phi(\|x - y_i\|_2) = \mathbf{f}(x_j), j = 1, 2, \ldots, , N_I \tag{44}$$

or

$$\mathcal{L}^I \alpha = \mathbf{F} \tag{45}$$

where

$$\mathcal{L}^I = [\mathcal{L}\phi(\|x - y_i\|_2)]_{N_I\times N} \tag{46}$$

At the points on the boundary, we impose boundary conditions as

$$\sum_{i=1}^{N} \alpha_i \mathcal{L}_B\phi(\|x - y_i\|_2) = \mathbf{g}(x_j), j = N_I + 1, \ldots, , N \tag{47}$$

or

$$\mathbf{B}\alpha = \mathbf{G} \tag{48}$$

where

$$\mathbf{B} = \mathcal{L}_B\phi\left[\left(\|x_{N_I+1} - y_j\|_2\right)\right]_{N_B \times N}$$

Therefore, we can write a finite-dimensional static problem as

$$\begin{bmatrix} \mathcal{L}^I \\ \mathbf{B} \end{bmatrix}\alpha = \begin{bmatrix} \mathbf{F} \\ \mathbf{G} \end{bmatrix} \tag{49}$$

By inverting the system (49), we obtain the vector $\boldsymbol{\alpha}$. We then obtain the solution $\mathbf{u}$ using the interpolation equation (42).

Discretization of the equations of motion and boundary conditions

The radial basis collocation method follows a simple implementation procedure. Taking equation (11), we compute

$$\alpha = \begin{bmatrix} L^I \\ \mathbf{B} \end{bmatrix}^{-1}\begin{bmatrix} \mathbf{F} \\ \mathbf{G} \end{bmatrix} \tag{50}$$

This $\boldsymbol{\alpha}$ vector is then used to obtain solution $\tilde{\mathbf{u}}$, by using (5). If derivatives of $\tilde{\mathbf{u}}$ are needed, such derivatives are computed as

$$\frac{\partial \tilde{\mathbf{u}}}{\partial x} = \sum_{j=1}^{N} \alpha_j \frac{\partial \phi_j}{\partial x} \tag{51}$$

$$\frac{\partial^2 \tilde{\mathbf{u}}}{\partial x^2} = \sum_{j=1}^{N} \alpha_j \frac{\partial^2 \phi_j}{\partial x^2}, \text{etc} \tag{52}$$

In the present collocation approach, we need to impose essential and natural boundary conditions. Consider, for example, the condition $w = 0$, on a simply supported or clamped edge. We enforce the conditions by interpolating as

$$w = 0 \rightarrow \sum_{j=1}^{N} \alpha_j^W \phi_j = 0 \tag{53}$$

Other boundary conditions are interpolated in a similar way.

Numerical examples

All numerical examples consider a Chebyshev grid and a Wendland function, defined as

$$\phi(r) = (1 - c\ r)_+^8 \left(32(c\ r)^3 + 25(c\ r)^2 + 8c\ r + 1\right) \tag{54}$$

where the shape parameter (c) was obtained by an optimization procedure, as detailed in Ferreira and Fasshauer [44].

Static problems-cross-ply laminated plates

A simply supported square laminated plate of side a and thickness h is composed of four equally layers oriented at [0°/90°/90°/0°]. The plate is subjected to a sinusoidal vertical pressure of the form

$$p_z = P \sin\left(\frac{\pi x}{a}\right) \sin\left(\frac{\pi y}{a}\right)$$

with the origin of the coordinate system located at the lower left corner on the midplane and P the maximum load (at center of plate).

The orthotropic material properties for each layer are given by

$$E_1 = 25.0E_2 \quad G_{12} = G_{13} = 0.5E_2 \quad G_{23} = 0.2E_2 \quad \nu_{12} = 0.25$$

The in-plane displacements, the transverse displacements, the normal stresses and the in-plane and transverse shear stresses are presented in normalized form as

$$\overline{w} = \frac{10^2 w_{(a/2,a/2,0)} h^3 E_2}{Pa^4} \quad \overline{\sigma}_{xx} = \frac{\sigma_{xx(a/2,a/2,h/2)} h^2}{Pa^2} \quad \overline{\sigma}_{yy} = \frac{\sigma_{yy(a/2,a/2,h/4)} h^2}{Pa^2}$$

$$\overline{\tau}_{xz} = \frac{\tau_{xz(0,a/2,0)} h}{Pa} \qquad \overline{\tau}_{xy} = \frac{\tau_{xy(0,0,h/2)} h^2}{Pa^2}$$

In Table 1 we present results for for the present ZZ theory, using 11×11 up to 21×21 points. We compare results with higher order solutions by Ahkras [45] , and Reddy [46], FSDT solutions by Reddy and Chao [47], and an exact solution by Pagano [48]. We also compare with results by the authors using RBFs with Reddy's theory [39], and a layerwise theory [49]. Our ZZ theory produces excellent results, when compared with other HSDT theories, for all a/h ratios, for transverse displacements, normal stresses and transverse shear stresses. In Figures 3 and 4 the σ_{xx} evolution across the thickness direction is illustrated, for $a/h = 4$, using 21×21 points, with load applied at the top surface and middle surface, respectively. In Figures 5 and 6 the τ_{xz} evolution across the thickness direction is illustrated,

Table 1. [0°/90°/90°/0°] square laminated plate under zig-zag formulation.

$\frac{a}{h}$	Method	$\overline{w}$	$\overline{\sigma}_{xx}$	$\overline{\sigma}_{yy}$	$\overline{\tau}_{zx}$	$\overline{\tau}_{xy}$
4	HSDT [46]	1.8937	0.6651	0.6322	0.2064	0.0440
	FSDT [47]	1.7100	0.4059	0.5765	0.1398	0.0308
	Elasticity [48]	1.954	0.720	0.666	0.270	0.0467
	Present (13 × 13 grid)	1.8930	0.6408	0.8506	0.2160	0.0437
	Present (17 × 17 grid)	1.8931	0.6408	0.8506	0.2160	0.0436
	Present (21 × 21 grid)	1.8931	0.6408	0.8506	0.2160	0.0436
10	HSDT [46]	0.7147	0.5456	0.3888	0.2640	0.0268
	FSDT [47]	0.6628	0.4989	0.3615	0.1667	0.0241
	Elasticity [48]	0.743	0.559	0.403	0.301	0.0276
	Present (13 × 13 grid)	0.7227	0.5460	0.4192	0.2978	0.0269
	Present (17 × 17 grid)	0.7227	0.5460	0.4194	0.2978	0.0269
	Present (21 × 21 grid)	0.7227	0.5460	0.4194	0.2978	0.0269
100	HSDT [46]	0.4343	0.5387	0.2708	0.2897	0.0213
	FSDT [47]	0.4337	0.5382	0.2705	0.1780	0.0213
	Elasticity [48]	0.4347	0.539	0.271	0.339	0.0214
	Present (13 × 13 grid)	0.4292	0.5360	0.2705	0.3340	0.0211
	Present (17 × 17 grid)	0.4293	0.5363	0.2700	0.3343	0.0211
	Present (21 × 21 grid)	0.4294	0.5363	0.2699	0.3344	0.0211

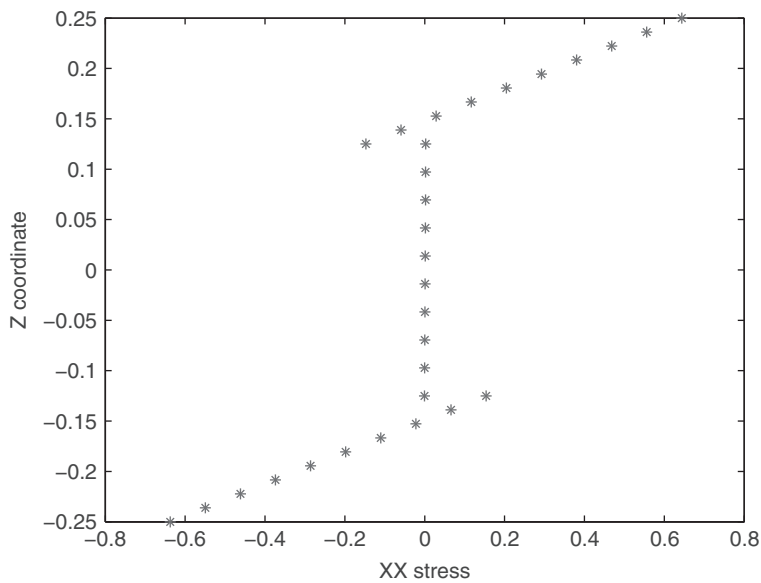

Figure 3. Normalized normal σ_{xx} stress for $a/h = 4$, 21 × 21 points, load at $z = h/2$.

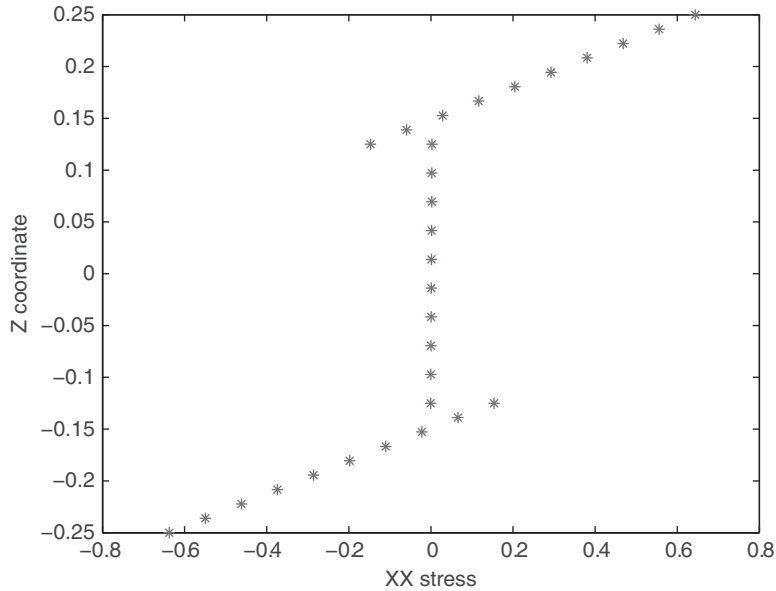

Figure 4. Normalized normal σ_{xx} stress for $a/h = 4$, 21×21 points, load at $z = 0$.

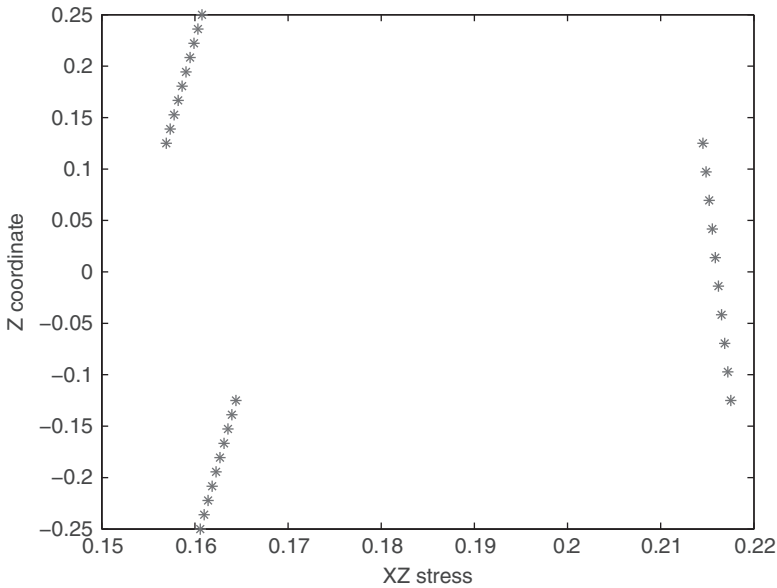

Figure 5. Normalized transverse τ_{xz} stress for $a/h = 4$, 21×21 points, load at $z = h/2$.

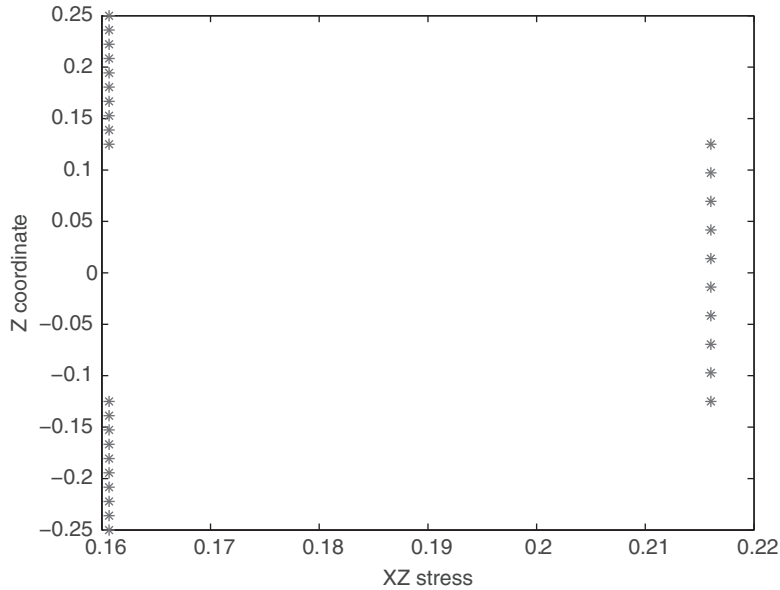

Figure 6. Normalized transverse τ_{xz} stress for $a/h = 4$, 21×21 points, load at $z = 0$.

for $a/h = 4$, using 21×21 points, with load applied at the top surface and middle surface, respectively. Note that the transverse shear stresses are obtained directly from the constitutive equations.

The load was applied at $z = h/2$ and $z = 0$. It is interesting to note the difference on the transverse shear stress, when loads are applied in the middle surface or on top surface.

Sandwich plate

In this example, we consider a simply-supported square sandwich plate loaded by uniform transverse pressure p. The length and thickness of the plate are denoted by a, h, respectively. The plate ratio a/h is taken as 10. It consists of a two skins with equal thickness ($0.1h$) with the following mechanical properties

$$E_1/E_2 = 25; \quad G_{12}/E_2 = G_{13}/E_2 = 0.5; \quad G_{23}/E_2 = 0.2; \quad \nu_{12} = 0.25 \tag{55}$$

while the inner layer, the weak core, has a thickness of $0.8h$ and the following mechanical properties:

$$E_1/E_2 = 1; \quad G_{13}/E_2 = G_{23}/E_2 = 0.06; \quad G_{12}/E_2 = 0.016; \quad \nu_{12} = 0.25 \tag{56}$$

Table 2. Load applied at $z = h/2$: square sandwich plates; Transverse displacements $U_z = (a/2, b/2, 0)$ and in-plane $S_{xx} = (a/2, b/2; h/2)$ and out-of-plane stress $S_{xz} = (0, b/2, 0)$

	$\bar{U}_z$			$\bar{S}_{xx}$			$\bar{S}_{xz}$		
a/h	4	10	100	4	10	100	4	10	100
13×13	10.6356	3.0549	1.2482	1.8904	1.4940	1.4978	0.4081	0.5183	0.5614
17×17	10.6424	3.0584	1.2474	1.8947	1.5005	1.4975	0.4078	0.5186	0.5702
21×21	10.6438	3.0591	1.2477	1.8954	1.5023	1.4981	0.4078	0.5188	0.5722
LM4	10.682	3.083	1.262	1.902	1.509	1.505	0.4074	0.5276	0.5889
EMZC3	10.678	3.082	1.262	1.899	1.507	1.504	0.3949	0.5239	0.5886
EMZC3d	10.626	3.026	1.230	1.915	1.480	1.476	0.4031	0.5224	0.5865
ED4	9.909	2.923	1.260	1.929	1.519	1.506	0.3574	0.5104	0.5881
ED1	5.542	1.982	1.218	1.145	1.388	1.475	0.5249	0.5716	0.5876
FSDT	5.636	1.984	1.218	1.168	1.391	1.476	0.5249	0.5716	0.5876
CLT	1.2103	1.2103	1.2103	1.476	1.476	1.476	0.5878	0.5878	0.5878

In Table 2 the present RBF formulation is compared with closed-form results by Carrera and Ciuffreda [50]. Results are normalized as

$$\bar{U}_z = \frac{U_z E_T 100 h^3}{q a^4}; \quad \bar{S}_{xx} = \frac{S_{xx} h}{q a}; \quad \bar{S}_{xz} = \frac{S_{xz} h}{q a}$$

It is clear that the CLT and FSDT are totally inadequate to model such sandwich structures. The present meshless implementation of the Murakami's ZZ theory seems to produce results of the highest quality in terms of the transverse displacement, normal and transverse shear stresses.

Conclusions

In this article we presented a study using the radial basis function collocation method to analyze static deformations of thin and thick sandwich plates using the MZZF, allowing for through-the-thickness deformations. This has not been done before and serves to fills the gap of knowledge in this area.

Using the UF with the radial basis collocation, all the C^o plate formulations can be easily discretized by radial basis functions collocation. Also, the burden of deriving the equations of motion and boundary conditions is eliminated with the present approach. All is needed is to change one vector F_t that defines the expansion of displacements.

We analyzed square sandwich plates in bending. The present results were compared with existing analytical solutions or competitive finite element solutions and excellent agreement was observed in all cases.

The present method is a simple yet powerful alternative to other finite element or meshless methods in the static deformation analysis of thin and thick sandwich plates.

Funding

The support of Ministério da Ciência Tecnologia e do Ensino superior and Fundo Social Europeu (MCTES and FSE) under programs POPH-QREN and project PTDC/EME-PME/109116/2008 are gratefully acknowledged.

References

1. Carrera E. Historical review of zig-zag theories for multilayered plates and shells. *Appl Mech Rev* 2003; 56: 287–308.
2. Kirchhoff G. Uber das gleichgewicht und die bewegung einer elastischen scheibe. *J Angew Math* 1850; 40: 51–88.
3. Reissner E. The effect of transverse shear deformations on the bending of elastic plates. *J Appl Mech* 1945; 12: A69–A77.
4. Mindlin RD. Influence of rotary inertia and shear in flexural motions of isotropic elastic plates. *J Appl Mech* 1951; 18: 31–38.
5. Zenkert D. *An introduction to sandwich structures*. Oxford: Chamelon Press, 1995.
6. Vinson JR. *The behavior of sandwich structures of isotropic and composite materials*. Lancaster, PA: Technomic Publishing Co., 1999.
7. Burton S and Noor AK. Assessment of computational model for sandwich panels and shells. *Comput Meth Appl Mech Eng* 1995; 124: 125–151.
8. Noor AK, Burton S and Bert CW. Computational model for sandwich panels and shells. *Appl Mech Rev* 1996; 49: 155–199.
9. Altenbach H. Theories for laminated and sandwich plates. a review. *Int Appl Mech* 1998; 34: 243–252.
10. Librescu L and Hause T. Recent developments in the modeling and behaviors of advanced sandwich constructions: a survey. *Compos Struct* 2000; 48: 1–17.
11. Vinson JR. Sandwich structures. *Appl Mech Rev* 2001; 54: 201–214.
12. Demasi L. 2d, quasi 3d and 3d exact solutions for bending of thick and thin sandwich plates. *J Sandwich Struct Mater* 2008; 10: 271–310.
13. Murakami H. Laminated composite plate theory with improved in-plane responses. *J Appl Mech* 1986; 53: 661–666.
14. Carrera E. Developments, ideas, and evaluations based upon reissner's mixed variational theorem in the modelling of multilayered plates and shells. *Appl Mech Rev* 2001; 54: 301–329.
15. Carrera E. The use of murakami's zig-zag function in the modeling of layered plates and shells. *Compos Struct* 2004; 82: 541–554.
16. Demasi L. ∞^3hierarchy plate theories for thick and thin composite plates: the generalized unified formulation. *Compos Struct* 2008; 84: 256–270.
17. Brischetto S, Carrera E and Demasi L. Improved bending analysis of sandwich plate by using zig-zag function. *Compos Struct* 2009; 89: 408–415.
18. Daya BS, Hu EM, H, et al. Evaluation of kinematic formulations for viscoelastically damped sandwich beam modeling. *J Sandwich Struct Mater* 2006; 8: 477–495.
19. Frostig Y. Bending of curved sandwich panels with transversely flexible core: Closed form higher-order theory. *J Sandwich Struct Mater* 1999; 1: 4–41.

20. Frostig Y and Rabinovich O. Behavior of unidirectional sandwich panels with a multi-skin construction or a multilayered core layout-higher- order approach. *J Sandwich Struct Mater* 2000; 2: 181–213.
21. Kansa EJ. Multiquadrics- a scattered data approximation scheme with applications to computational fluid dynamics. I: Surface approximations and partial derivative estimates. *Comput Math Appl* 1990; 19(8/9): 127–145.
22. Hon YC, Lu MW, Xue WM, et al. Multiquadric method for the numerical solution of byphasic mixture model. *Appl Math Comput* 1997; 88: 153–175.
23. Hon YC, Cheung KF, Mao XZ, et al. A multiquadric solution for the shallow water equation. *ASCE J Hydraul Eng* 1999; 125(5): 524–533.
24. Wang JG, Liu GR and Lin P. Numerical analysis of biot's consolidation process by radial point interpolation method. *Int J Solid Struct* 2002; 39(6): 1557–1573.
25. Liu GR and Gu YT. A local radial point interpolation method (lrpim) for free vibration analyses of 2-d solids. *J Sound Vibr* 2001; 246(1): 29–46.
26. Liu GR and Wang JG. A point interpolation meshless method based on radial basis functions. *Int J Numer Meth Eng* 2002; 54: 1623–1648.
27. Wang JG and Liu GR. On the optimal shape parameters of radial basis functions used for 2-d meshless methods. *Comput Meth Appl Mech Eng* 2002; 191: 2611–2630.
28. Chen XL, Liu GR and Lim SP. An element free galerkin method for the free vibration analysis of composite laminates of complicated shape. *Compos Struct* 2003; 59: 279–289.
29. Dai KY, Liu GR, Lim SP, et al. An element free galerkin method for static and free vibration analysis of shear-deformable laminated composite plates. *J Sound Vibr* 2004; 269: 633–652.
30. Liu GR and Chen XL. Buckling of symmetrically laminated composite plates using the element-free galerkin method. *Int J Struct Stabil Dynam* 2002; 2: 281–294.
31. Liew KM, Chen XL and Reddy JN. Mesh-free radial basis function method for buckling analysis of non-uniformity loaded arbitrarily shaped shear deformable plates. *Comput Meth Appl Mech Eng* 2004; 193: 205–225.
32. Huang YQ and Li QS. Bending and buckling analysis of antisymmetric laminates using the moving least square differential quadrature method. *Comput Meth Appl Mech Eng* 2004; 193: 3471–3492.
33. Liu L, Liu GR and Tan VCB. Element free method for static and free vibration analysis of spatial thin shell structures. *Comput Meth Appl Mech Eng* 2002; 191: 5923–5942.
34. Xiang S, Wang KM, Ai YT, et al. Analysis of isotropic, sandwich and laminated plates by a meshless method and various shear deformation theories. *Compos Struct* 2009; 91(1): 31–37.
35. Xiang S, Shi H, Wang KM, et al. Thin plate spline radial basis functions for vibration analysis of clamped laminated composite plates. *Eur J Mech A/Solids* 2010; 29: 844–850.
36. Roque FAJA, CMC and Jorge RMN. Analysis of composite and sandwich plate by trigonometric layer-wise deformation theory and radial basis function. *J Sandwich Struct Mater* 2006; 8: 497–515.
37. Ferreira AJM. A formulation of the multiquadric radial basis function method for the analysis of laminated composite plates. *Compos Struct* 2003; 59: 385–392.
38. Ferreira AJM. Thick composite beam analysis using a global meshless approximation based on radial basis functions. *Mech Adv Mater Struct* 2003; 10: 271–284.
39. Ferreira AJM, Roque CMC and Martins PALS. Analysis of composite plates using higher-order shear deformation theory and a finite point formulation based on the multiquadric radial basis function method. *Compos Part B* 2003; 34: 627–636.

40. Carrera E. C^0reissner-mindlin multilayered plate elements including zig-zag and interlaminar stress continuity. *Int J Numer Meth Eng* 1996; 39: 1797–1820.
41. Carrera E and Kroplin B. Zig-zag and interlaminar equilibria effects in large deflection and post-buckling analysis of multilayered plates. *Mech Compos Mater Struct* 1997; 4: 69–94.
42. Carrera E. Evaluation of layer-wise mixed theories for laminated plate analysis. *AIAA J* 1998; 36): 830–839.
43. Hardy RL. Multiquadric equations of topography and other irregular surfaces. *Geophys Res* 1971; 176: 1905–1915.
44. Ferreira AJM and Fasshauer GE. Computation of natural frequencies of shear deformable beams and plates by a rbf-pseudospectral method. *Comput Meth Appl Mech Eng* 2006; 196: 134–146.
45. Akhras G, Cheung MS and Li W. Finite strip analysis for anisotropic laminated composite plates using higher-order deformation theory. *Comput Struct* 1994; 52(3): 471–477.
46. Reddy JN. A simple higher-order theory for laminated composite plates. *J Appl Mech* 1984; 51: 745–752.
47. Reddy JN and Chao WC. A comparison of closed-form and finite-element solutions of thick laminated anisotropic rectangular plates. *Nucl Eng Des* 1981; 64: 153–167.
48. Pagano NJ. Exact solutions for rectangular bidirectional composites and sandwich plates. *J Compos Mater* 1970; 4: 20–34.
49. Ferreira AJM. Analysis of composite plates using a layerwise deformation theory and multiquadrics discretization. *Mech Adv Mater Struct* 2005; 12(2): 99–112.
50. Carrera E and Ciuffreda A. A unified formulation to assess theories of multilayered plates for various bending problems. *Compos Struct* 2005; 69: 4271–293.